Vehicular ammonia emissions: An underappreciated emission source in densely-populated areas

Yifan Wen[1], Shaojun Zhang[1, 2, 3*], Ye Wu[1, 2, 3], Jiming Hao[1, 2, 3]

[1]School of Environment, State Key Joint Laboratory of Environment Simulation and Pollution Control, Tsinghua University, Beijing, 100084, China
[2]State Environmental Protection Key Laboratory of Sources and Control of Air Pollution Complex, Beijing, 100084, China
[3]Beijing Laboratory of Environmental Frontier Technologies, School of Environment, Tsinghua University, Beijing 100084, China

Correspondence to: Shaojun Zhang (zhsjun@tsinghua.edu.cn)

Abstract. On-road ammonia (NH_3) emissions play a significant role in fine particulate matter ($PM_{2.5}$) formation in urban areas, posing severer risks for human health. Limited studies have depicted the spatial and temporal variations of on-road NH_3 emissions, in particular lacking detailed quantification of their contributions within densely-populated areas. In this study, we established a comprehensive vehicular NH_3 emission model and compiled a gridded on-road NH_3 emission inventory with high spatial (3 km × 3 km), and temporal (monthly) resolutions for mainland China. China's annual vehicular NH_3 emissions are estimated to increase from 32.8±1.7 kt to 87.1±37.5 kt during the period of 2000-2019. Vehicular NH_3 emissions are significantly concentrated in densely-populated areas where agricultural emissions have relatively lower intensity. It is found that vehicular NH_3 emissions could exceed agricultural emissions in the grids containing 23.0±2.1% of the Chinese population in 2019 (approximately 326.6±25.4 million people), and this ratio is up to 29.4±3.0% in winter. For extreme populous megacities such as Beijing and Shanghai, vehicular NH_3 emissions exceed agricultural emissions where 69.2±1.2% and 72.0±1.3% of population resides, respectively. Thus, the significant role of on-road NH_3 emissions in populated areas may have been underappreciated. This study gave a better insight into the absolute value and relative importance of on-road NH_3 emissions in different regions, seasons and population densities in China, which is important in terms of the air quality implications.

1 Introduction

As the leading alkaline gas and one of the major reactive nitrogen species in the atmosphere, ammonia (NH_3) plays a vital role in fine particulate matter ($PM_{2.5}$) pollution and nitrogen deposition. NH_3 readily neutralizes with acidic species from sulfur dioxide (SO_2) and nitrogen oxides (NO_X) precursors to form secondary organic aerosols (SOA) (Lv et al., 2022; Chu et al., 2016), which not only enhances regional haze but also threatens public health (Huang et al., 2014; Ru-Jin et al., 2014; Pan et al., 2016). It is found that NH_3 emissions contributed larger to $PM_{2.5}$ than NOx emission globally and in most countries, indicating that $PM_{2.5}$ is more strongly NH_3-limited than NO_X-limited (Gu et al., 2021). There are increasing evidences

indicating that the reduction of NH_3 emissions should be more efficient than other particle precursors at mitigating haze pollution (Fu et al., 2017; Gu et al., 2021), highlighting the priority for ammonia regulation. After removal from atmosphere, NH_3 and ammonium (NH_4^+) from both wet and dry deposition may also contribute to soil acidification, eutrophication, and even to a reduction of biodiversity (Stevens et al., 2004; Li et al., 2016). Therefore, efforts to better understand and control

35   NH_3 emissions are essential.

Although agriculture dominates the total anthropogenic NH_3 emissions at global scales (Paulot et al., 2014), increasing studies have pointed out the significant role of on-road NH_3 emissions in urban areas (Chang et al., 2016; Farren et al., 2020; Fenn et al., 2018; Sun et al., 2017b). On-road NH_3 emissions are highly concentrated in densely-populated areas where agricultural emissions rarely exist (Sun et al., 2017a). It is reported that on-road NH_3 emissions have exceeded agricultural emissions where

40   nearly half the U.S. population resides (Sun et al., 2017a; Fenn et al., 2018). Pronounced bimodal diurnal variations in NH_3 concentration consistent with traffic patterns were also observed in many megacities, suggesting a significant contribution of on-road NH_3 emissions in urban areas (Wang et al., 2015; Pandolfi et al., 2012). Moreover, on-road NH_3 emissions are co-emitted with NO_X in dense, highly urbanized areas, and may have a more effective pathway to particle formation than agricultural NH_3 emitted in rural, low-NO_X areas (Farren et al., 2020). Thus, on-road NH_3 emissions could be critical for public

45   health in urban areas due to their contribution to $PM_{2.5}$ formations, since more than half of the global populations live within cities (World Bank Group, 2022).

There are two major sources for vehicular NH_3 emissions - gasoline vehicles equipped with three-way catalysts (TWC) and diesel vehicles equipped with selective catalytic reduction (SCR). NH_3 is the by-product from the reduction of nitric oxide (NO) for gasoline vehicles equipped with TWC (Livingston et al., 2009; Bishop and Stedman, 2015). Also, NH_3 leakage during

50   the injection of urea to SCR system, commonly termed "ammonia slip", is gaining importance with the extensive applications of SCR in diesel vehicles (Suarez-Bertoa et al., 2017; Mendoza-Villafuerte et al., 2017; He et al., 2020). With the extensive equipment of TWCs and SCR for the latest emission standards, NH_3 contributes increasing fractions of the reactive nitrogen species emitted by vehicles in the recent decade (Bishop et al., 2010; Sun et al., 2017b; Fenn et al., 2018). However, regulations for on-road NH_3 emissions are far behind other traffic-related pollutants (i.e., NO_X, PM, CO and HC) (Wu et al., 2017b).

55   Currently, the heavy-duty Euro/China VI is the only emission standard legislates an NH_3 emission cap (10 ppm as the cycle-average slip limit) aiming at restrain SCR slip (Sun et al., 2017a). To response the increasing concern regarding vehicular NH_3 emissions, stringent limits of 20 mg/km for light-duty vehicles and 65 mg/kWh for heavy-duty vehicles have been introduced in a proposal version of future Euro 7/VII regulations (European Commission, 2022). The introduction of NH_3 emission limits the installation will require installation of specific after-treatment devices; for example, ammonia slip catalysts (ASC) and

60   Clean Up Catalyst (CUC) are expected to ensure Euro 7/VII vehicles to comply with these proposed limits (Torp et al., 2021). NH_3 emission inventories can significantly affect the accuracy of $PM_{2.5}$ modeling and play a crucial role in the refinement of mitigation strategies. Numerous studies have established NH_3 emission inventories on global level (Meng et al., 2017), national level (Fenn et al., 2018; Xing et al., 2013; Kang et al., 2016; Li et al., 2021), and regional level (Zhao et al., 2012; Zheng et al., 2012). However, these studies failed to take into account the spatial distribution of on-road NH_3 emissions and the potential

65 for relatively higher emissions from mobile sources in dense, highly urbanized areas. Also, NH_3 emissions from the transportation sector are thought to be highly underestimated in global (Meng et al., 2017), the US (Sun et al., 2017b) and UK (Farren et al., 2020), mainly due to the large uncertainties remain in vehicular NH_3 emission factors (EF) and traffic activity data (Meng et al., 2017). The exact contribution of traffic sources to NH_3 emissions in various spatial scales is still an area of debate, especially in densely-populated areas. Therefore, comprehensive vehicular NH_3 EFs and high quality on-road NH_3

70 emission inventories are urgently required for air quality modelling and future NH_3 regulations.

In this study, we established a comprehensive vehicular NH_3 emission factor (EF, unit in mg/km) model including both gasoline and diesel vehicles. The long-term trend of vehicular NH_3 emissions from 2000 to 2019 was estimated based on the EF factors and province-level traffic activity data. Then a highly-resolved vehicular NH_3 emission inventory with high spatial (3 km×3 km) and temporal (monthly) resolutions was compiled for mainland China, and the relative contribution of on-road

75 vehicles to total anthropogenic NH_3 emissions were analyzed among different seasons and population densities. This study is aimed to give a better insight into the absolute value and relative importance of on-road NH_3 emissions in different regions, seasons and population density, which is important in terms of the air quality implications.

2 Methodology and data

2.1 Establishment of vehicular NH_3 emission factor model

80 We developed a comprehensive vehicular NH_3 EF model for both gasoline and diesel vehicles based on the local exhaust measurement data in China. Nine vehicle categories and six emission standards (i.e., China 1/I to China 6/VI) were divided according to the official vehicle registration rules in China (see Table S1).

For gasoline vehicles, Huang et al (Huang et al., 2018) revealed the strong correlation between NH_3 emissions and modified combustion efficiency (MCE), an indicator calculated based on CO and CO_2 emissions. In this study, CO and CO_2 EFs for

85 gasoline vehicles were obtained from EMBEV model, the archetype model for China's National Emission Inventory Guidebook (Zhang et al., 2014). Several studies have found significant temperature-dependence for NH_3 emissions from light-duty gasoline vehicles (LDGVs) that increased as the temperature decreased, mainly linked to rich combustion during cold-start operations (Selleri et al., 2022; Suarez-Bertoa et al., 2017). The latest version of EMBEV updated the cold-start sub-module and developed comprehensive ambient temperature corrections that can characterize the spatial and monthly variations

90 in EFs across China (Wen et al., 2021), enable us to estimate NH_3 EFs under various seasons and provinces.

For diesel vehicles, we obtained NH_3 measurement data from a fleet of heavy-duty diesel vehicles (HDDVs) (China III to China V) using PEMS and dynamometer (He et al., 2020). As China VI has not been widely implemented until 2020, the NH_3 EFs for HDDVs were categorized into pre-China IV (without SCR) and China IV/V (majorly equipped with SCR). The test results indicated that the introduction of SCR systems to diesel fleets might risk higher NH_3 emissions, though NH_3 emissions

95 varied significantly among tested HDDVs. NH_3 EFs of other diesel vehicles were calculated based on the relative fuel consumptions comparing with HDDVs. We did not introduce temperature corrections due to the lack of measurements.

As for the uncertainties in NH$_3$ EFs, we referred to the error bars of NH$_3$ emission measurements from various studies (Table S2 and S3) to estimate the uncertainty ranges of gasoline and diesel vehicles under different emission standards, shown in Table S4. For diesel vehicles, the large uncertainty ranges in SCR-equipped EFs have involved the impacts of abnormal urea uses and different SCR control strategies.

2.2 Bottom-up estimation of long-term vehicular NH$_3$ emissions

In this study, vehicular NH$_3$ emissions inventories by province and month were calculated for mainland China from 2000 to 2019 based on a bottom-up method, involving vehicle population, vehicle kilometer traveled (VKT), and NH$_3$ EFs by province, calendar year, month and vehicle category, as Eq. (1) illustrates.

$$E_{p,y,m} = \sum_{v}\sum_{f}\sum_{es} VP_{v,f,es,p,y} \times VKT_{v,f,es,p,y} \times EF_{v,f,es,p,m} \times 10^{-9} \tag{1}$$

where $E_{p,y,m}$ is the monthly vehicular NH$_3$ emissions of province p in calendar year y from 2000 to 2019, units in t; $VP_{v,f,es,p,y}$ is the vehicle population of province p in calendar year y, defined by vehicle category v, fuel type f, and emission standard es, units in veh; $VKT_{v,f,es,p,y}$ is the corresponding annual-average VKT, units in km/year; $EF_{v,f,es,p,m}$ is the NH$_3$ EFs in province p and month m, defined by vehicle category v, fuel type f, and emission standard es, units in mg/km. The province-level vehicle populations were obtained from National Bureau of Statistics of China (NBSC) and further processed to match up with the resolution and scale of this study (method reported by Wu et al. (Wu et al., 2016)). The annual-average VKT for various vehicle categories was estimated based on previous survey results regarding vehicle usage in China (Wu et al., 2016; Wu et al., 2017a; Zhang et al., 2014). The NH$_3$ EFs by province, month and vehicle category are obtained from the vehicular NH$_3$ emission factor model established in 2.1.

To validate the accuracy of bottom-up estimations, we compared the NH$_3$ emissions from gasoline vehicles with the top-down estimation based on annual gasoline consumption and fuel-based EFs from related studies, as Eq. (2) illustrates.

$$E_{top-down,y} = FC_y \times 0.85 \times \frac{M(CO_2)}{M(C)} \times EF_y\left(NH_3/CO_2\right) \times \frac{M(NH_3)}{M(CO_2)} \tag{2}$$

where, $E_{top-down,y}$ is the top-down estimation of NH$_3$ emissions from gasoline vehicles in calendar year y, units in t; FC_y is the annual gasoline consumption in calendar year y, units in t; FC_y is then converted to CO$_2$ emissions based on the carbon content (0.85 g/kg) of gasoline and the molar mass ratio of CO$_2$ and carbon; $EF_y\left(NH_3/CO_2\right)$ is the fuel-based NH$_3$ EFs of gasoline fleet in China in calendar year y from Sun et al (Sun et al., 2017b), units in ppbv/ppmv CO$_2$; $M(CO_2)$, $M(C)$ and $M(NH_3)$ are the molar masses of CO$_2$, carbon and NH$_3$, respectively, units in g/mol. The annual gasoline consumption data were obtained from National Bureau of Statistics of China (NBSC).

2.3 Compilation of the gridded NH$_3$ emission inventories

125 NH$_3$ emission data from other anthropogenic sources by province were obtained from the updating works of Zheng et al (Zheng et al., 2019). The agricultural and vehicular NH$_3$ emissions were compiled at 3 km×3 km and monthly resolutions for mainland China in 2019. Monthly variations in agricultural emissions referred to Zhang et al (Zhang et al., 2018). Emissions from fertilizer applications and livestock productions were presented at the provincial level first and then allocated by grassland areas and rural residential areas, referring to Li et al (Li et al., 2021). The land cover data with a resolution of 1 km was

130 obtained from China's National Land Use and Cover Change (CNLUCC) dataset (Xu et al., 2018).

For on-road NH$_3$ emissions, we allocated the total vehicular NH$_3$ emissions of each province to 3 km×3 km grids based on the relative ratio of traffic indicator in each grid (see Eq. (3) and (4)).

$$E_{p,i} = \frac{R_{traffic,i}}{\sum_1^n R_{traffic,i}} \times E_p \tag{3}$$

$$R_{traffic,i} = \left(a \cdot L_{rank1,i} + b \cdot L_{rank2,i} + c \cdot L_{rank3,i}\right) \times \left[d \cdot R_{urbanarea,i} + e \cdot \left(1 - R_{urbanarea,i}\right)\right] \tag{4}$$

135 where, i represents grid ID, p represents province, n is the grid number in each province; E_p is the total vehicular NH$_3$ emissions of province p in 2019, units in t; $E_{p,i}$ is the vehicular NH$_3$ emissions allocated to grid i, units in t; $R_{traffic,i}$ is the traffic indicator in grid i, defined by road length of different road types ($L_{rank,i}$, rank1-3 represents for highway, arterial road and residential road) and the urban area ratio ($R_{urbanarea,i}$); a-e are allocating factors, referring to the traffic flow ratio of different road types in urban and rural areas in Beijing (Yang et al., 2019). Here, a-e are 1, 0.4, 0.3, 0.8, and 0.2, respectively. The digital road map

140 was obtained from the latest OpenStreetMap data for China (Openstreetmap, 2022). Urban area ratio was calculated based on the urban residential areas within each grid.

We compared the gridded allocation results of on-road NH$_3$ emissions with the estimations based on link-level inventories in four megacities in China (i.e., Beijing (Yang et al., 2019), Shanghai (An et al., 2021), Shenzhen (Wen et al., 2020) and Chengdu (Wen et al., 2022b)), shown in Fig S1. Link-level NH$_3$ emission inventories were calculated based on the traffic profiles of the

145 whole road network obtained in our previous studies (Wen et al., 2022a; Wen et al., 2020; Yang et al., 2019) and NH$_3$ EFs derived in 2.1. The coefficient of determination (R^2) varied from 0.63 to 0.80 among four megacities, demonstrating the accuracy of the allocation method for on-road emissions. We also compared the monthly variations of total anthropogenic NH$_3$ emissions derived in this study with surface NH$_3$ observations obtained from the Ammonia Monitoring Network in different regions of China in Kong et al (Kong et al., 2019), shown in Fig S2. The monthly variations compare well with NH$_3$

150 observations over different regions in China, demonstrating the accuracy of both spatial and monthly allocations.

3 Results and Discussion

3.1 Historical trend of vehicular NH$_3$ emissions in China

NH$_3$ EFs of LDGVs and HDDVs derived in this study are compared with relative literatures conducted by dynamometer, remote sensing, PEMS and other field measurements, as shown in Fig 1 (details listed in Table S2 and S3). NH$_3$ EFs of LDGVs decreased significantly with the upgrading of vehicle emission standards, consistent with trends in other literatures. Note the derivations of mg/km EFs from g/kg EFs have not been adjusted to account for different driving conditions/fuel consumption (see notes of Table S2 and S3), whilst dynamometer measurements may be lower than on-road emissions. Also impacts of various ambient environment and driving conditions, and interferences from high-emitter or other vehicle types may account for the differences (Davison et al., 2020). NH$_3$ EFs of HDDVs without SCR are negligible (4.4 ± 2.4 mg/km), while the introduction of SCR systems greatly increased the risks of ammonia slip (73.9 ± 118.7 mg/km). The introduction of Ammonia Slip Catalyst (ASC) in heavy-duty China VI emission standard would significantly reduce NH$_3$ emissions of HDDVs (Mendoza-Villafuerte et al., 2017). Since China VI HDDVs have not been deployed nationwide until Jul 2021, HDDVs equipped with SCR+ASC were not included in the calculation of NH$_3$ emission inventories.

Taking the phase in of emission standards into consideration, the trends of annual and fleet average NH$_3$ EFs for gasoline and diesel vehicles in China from 2000 to 2019 are shown in Fig S3. NH$_3$ EFs for gasoline vehicles decreased from 66.6±2.6 mg/km in 2000 to 16.0±3.9 mg/km in 2019 due to the continuously upgrading of emission standards. NH$_3$ EFs of diesel fleet were negligible before 2014, while started to increase with the national implementation of China IV in 2014. Fleet average NH$_3$ EF of diesel vehicles has surpassed gasoline vehicles in 2016 and increased to 36.5±29.2 mg/km in 2019.

The annual vehicular NH$_3$ emissions increased from 32.8±1.7 kt/yr to 87.1±37.5 kt/yr from 2000 to 2019 in China, as shown in Fig 2. The continuously increase from 2000 to 2010 mainly resulted from the rapid growth of gasoline vehicle ownership. However, emissions from gasoline vehicles started to decrease with the upgrading of emission standards in the past decade. NH$_3$ emissions of gasoline vehicles estimated based on bottom-up method agreed well with the top-down estimations based on annual gasoline consumption and fuel-based EFs (see Fig S4). Emissions from diesel vehicles grew significantly under the joint effects of increasing HDDV populations and the rapid introduction of SCR systems since 2014. The emission proportion of diesel fleet grew significantly from less than 3±2% before 2014 to 33±26% in 2019. With the implementation of heavy-duty China VI emission standard in 2020, NH$_3$ emissions from diesel vehicles should be well controlled. Gasoline vehicles (mainly LDGVs) will keep dominating the total on-road NH$_3$ emissions in the near future.

3.2 Spatial and temporal distributions of on-road NH$_3$ emissions in China

Highly spatial-resolved (3 km×3 km) vehicular NH$_3$ emission intensities in China in 2019 are illustrated in Fig 3. On-road emissions are distributed along road network, and the emission hotpots are highly correlated with densely-populated areas, which is different from the spatial distribution of agricultural emissions (see Fig S5). On-road NH$_3$ emission in two of the most populous regions, i.e., Beijing-Tianjin-Hebei (BTH) region, and the Yangtze River Delta (YRD) are also illustrated in Fig 3

(b) and (c). The average on-road NH_3 emission intensities in mainland China, BTH and YRD are 9.3±4.0, 42.4±18.2 and 46.5±20.0 kg·km^{-2}·yr^{-1}, with average population densities of 146, 511, and 668 person·km^{-2} in 2019, respectively. Note that on-road NH_3 emissions are positive correlated with population density, which will be further analyzed in 3.3.

We analyzed the contribution of on-road NH_3 emissions in total anthropogenic emissions in 2019. Agriculture (including livestock and fertilizer) dominated the total anthropogenic NH_3 nationwide (>90%), and the contribution of vehicular NH_3 emissions is insignificant comparing with agricultural emissions (<1%). However, the proportion of vehicular emissions varied significantly (from 0.36±0.16% to 8.91±3.83%) among provinces (see Fig S6). Beijing and Shanghai are the top two provinces with the highest vehicular NH_3 emission contributions in China, which are 8.91±3.83% and 7.33±3.15%, respectively, comparing with the nationwide level of 0.95±0.42%. Beijing and Shanghai are not only the core cities for BTH and YRD regions, but also two of the most populous megacities in China (with residential populations over 20 million). Thus, we chose Beijing and Shanghai as typical cities to discuss hereinafter.

Though several studies have pointed out the significant temperature-dependence of NH_3 emissions from LDGVs (Selleri et al., 2022; Suarez-Bertoa et al., 2017), few studies have considered the seasonal variation of on-road NH_3 emissions in either inventory or air quality modeling. In this study, the temperature impacts on NH_3 emissions have been depicted by the comprehensive EF model. Fig 4 illustrates the monthly variations in NH_3 EFs for LDGVs of various emission standards in Beijing and Shanghai. The fleet average NH_3 EFs of gasoline vehicles in February were 1.50 and 1.41 times of those in August for Beijing and Shanghai, respectively, consistent with the NH_3 emission ratio of 1.4~2.1 reported in dynamometer measurements conducted under -7 °C relative to 23 °C (Selleri et al., 2022; Suarez-Bertoa et al., 2017). As the monthly variations of agricultural emissions (higher in summer than winter) are opposite to vehicular emissions, the vehicle emission proportions are significantly higher in winter. As shown in Fig S7, the city-scale vehicular NH_3 emission proportions are up to 14% and 12% in winter in Beijing and Shanghai, respectively, nearly twice of the annual average ratio of 8.9% and 7.3%. The proportion would be even larger in urban areas, posing substantial risks for haze episodes during the wintertime.

3.3 Relative contribution of on-road and agricultural NH_3 emissions among different population density

The highly spatial-resolved NH_3 emission inventory enables us to distinguish the relative contribution of vehicular and agricultural emissions among various population densities. Population density data in mainland China were extracted from WorldPop (Tatem, 2017) at a spatial resolution of 100 m, then aggregated into 3 km to match the resolution of emission inventories. As shown in Fig 5, the distribution of on-road NH_3 emission intensity is positive correlated with population density, while the trend in agricultural emission is opposite. NH_3 emission intensities of on-road traffic are much lower than agriculture for less populated areas, but the median will surpass agricultural sources in grids with population density higher than 10 thousand person/km^2. For extreme populous grids (population density>20 thousand person/km^2), agricultural emissions are less important comparing with on-road traffic emissions.

According to the statistics based on gridded emission inventories and population density, on-road NH_3 emissions exceed agricultural emissions in grids containing 23.0±2.1% of the Chinese population in 2019 (approximately 326.6±25.4 million

people), and this number is up to 29.4±3.0% in winter. For densely-populated areas with population density higher than 2000 person/km^2, on-road NH$_3$ emissions exceed agricultural emissions where 53.3±3.6% of the population resides (approximately 287.8±19.5 million people), and up to 66.2±3.1% in winter. As two of the most populous megacities in the world, Beijing and Shanghai has 21.9 and 24.8 million residents in 2019. As shown in Fig 6, on-road NH$_3$ emissions in Beijing and Shanghai are significantly concentrated in densely-populated areas where agricultural emissions seldom exist, and gasoline vehicles accounted for most of these emissions due to the strict restrictions of heavy-duty trucks in central urban areas. The statistics show that on-road NH$_3$ emissions exceed agricultural emissions where 69.2±1.2% and 72.0±1.3% of population resides in Beijing and Shanghai, respectively. Thus, the significant role of on-road NH$_3$ emissions in populated areas and in winter may have been underappreciated without taking into account the temporal and spatial variations of on-road emission inventories. Note that residential emissions also serve as an important source for anthropogenic NH$_3$ emissions in Beijing and Shanghai (see Fig S7). However, residential NH$_3$ emissions (i.e., mainly from human excrement and domestic fuel combustion) are mostly attributed to human activities in rural residential areas for megacities like Beijing and Shanghai (Streets et al., 2003). Thus, even with high emission contributions in the whole city, residential emissions may not be as influential as traffic emissions in urban areas. As another important reactive nitrogen species besides NO$_X$, the significance of NH$_3$ emission control has not been fully addressed. Serving as a major contributor to both NO$_X$ and NH$_3$ emissions in urban areas, multipollutant control strategy for vehicular NO$_X$ and NH$_3$ emissions may be a more effective pathway to mitigate PM$_{2.5}$ pollution in densely-populated areas.

4 Conclusions

In this study, we established a comprehensive vehicular NH$_3$ emission factor model and compiled a gridded on-road NH$_3$ emission inventory with high spatial (3 km × 3 km), and temporal (monthly) resolutions for mainland China. NH$_3$ EFs for gasoline vehicles decreased from 66.6 mg/km in 2000 to 16.0 mg/km in 2019 due to the continuously upgrading of emission standards. The annual vehicular NH$_3$ emissions increased from 32.8±1.7 kt/yr to 87.1±37.5 kt/yr from 2000 to 2019 in China, mainly resulted from the rapid growth of gasoline vehicle ownership. On-road NH$_3$ emissions are significantly concentrated in densely-populated areas where agricultural emissions seldom exist. It is found that on-road NH$_3$ emissions exceed agricultural emissions in grids containing 23.0±2.1% of the Chinese population in 2019 (approximately 326.6 million people), and this ratio is up to 29.4±3.0% in winter. For extreme populous cities such as Beijing and Shanghai, on-road NH$_3$ emissions exceed agricultural emissions where 69.2±1.2% and 72.0±1.3% of population resides, respectively.

This study gave a better insight into the absolute value and relative importance of on-road NH$_3$ emissions in different regions, seasons and population densities in China, which is important in terms of the air quality implications. We emphasized the significant role of on-road NH$_3$ emissions in populated urban areas which may be underappreciated previously, highlighting the necessity to consider vehicular NH$_3$ emissions in air quality simulations. In addition, we clearly depicted the seasonal variation of on-road NH$_3$ emissions in our inventory by considering temperature-dependence of NH$_3$ emissions from LDGVs.

As the monthly variations of agricultural emissions (higher in summer than winter) are opposite to vehicular emissions (higher in winter than summer), the city-scale vehicular NH_3 emission proportions in winter are nearly twice of the annual average ratio in Beijing and Shanghai. This finding reminds us of the possibly more severe risks for haze episodes during the wintertime. Precise air quality simulations based on the highly-resolved NH_3 emission inventory are required to quantify the relative contribution of on-road NH_3 emissions to urban $PM_{2.5}$ pollution in different seasons.

Although several pathways for agricultural emission abatement have been raised (Sha et al., 2021), the regulation for agricultural NH_3 emissions is difficult due to both the technical gap and potential obstruction from stakeholders (Plautz, 2018). However, mitigating vehicular NH_3 emissions could be more feasible compared with the control of agricultural emissions. With the implementation of heavy-duty Euro/China VI emission standard, NH_3 emissions from diesel vehicles are expected to be well-controlled (see Fig 1). The NH_3 emission problems from petrol vehicles have also been addressed by the coming Euro 7/VII standard (European Commission, 2022), and there are proven aftertreatments to ensure Euro 7/VII vehicles comply with these proposed limits (Torp et al., 2021). Except for regulations from emission standards, traffic management for passenger vehicle fleet and promotion of electric vehicles can also significantly mitigate vehicular NH_3 emissions in urban areas. Therefore, the control of on-road NH_3 emissions can be a feasible and cost-effective way for mitigating haze pollution in urban areas, calling for great priority to strengthen regulations for vehicular NH_3 emissions worldwide.

Note there are some limitations about this study. Firstly, impacts of driving condition were not included in this study. It's well documented that LDGV NH_3 emissions are strongly dependent on driving conditions (Huang et al., 2018). Higher LDGV NH_3 emissions are found under both low-speed (Farren et al., 2021) and aggressive highway driving cycles (Huang et al., 2018). For urban areas with complex driving conditions and easily affected by traffic congestion, vehicular NH_3 emissions can be further enhanced. It's important to address the impacts of traffic conditions on vehicular NH_3 emissions in urban areas if real-world speed monitoring data is available in future works (Wang et al., 2023). Secondly, we estimated EFs of other diesel vehicles based on the relative fuel consumptions compared with HDDVs due to the lack of measurement data. This approach has obvious limitations and can be improved if more measurement data are available. Nevertheless, HDDVs accounted for 89.8% of the total NH_3 emissions from diesel vehicles in 2019. Thus, the uncertainties brought by EFs of other diesel vehicles are limited.
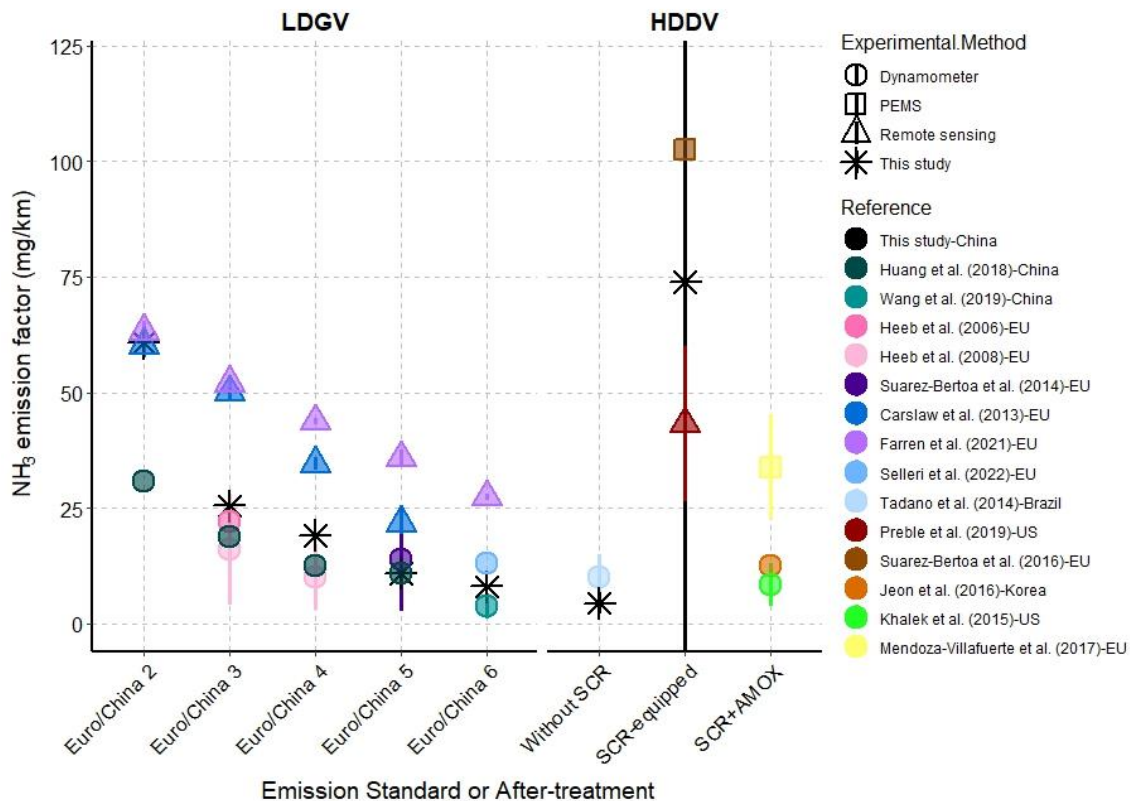
Figure 1: Comparison of distance-based NH₃ EFs for of LDGVs and HDDVs in this study and other relative studies, disaggregated by emission standard or after-treatment technology.
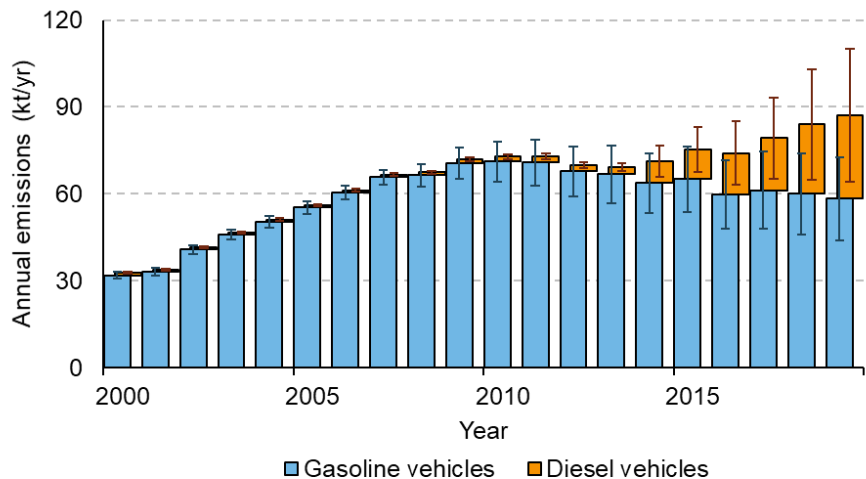
Figure 2: Annual vehicular NH₃ emissions by fuel type in China with uncertainty ranges, 2000-2019.

280
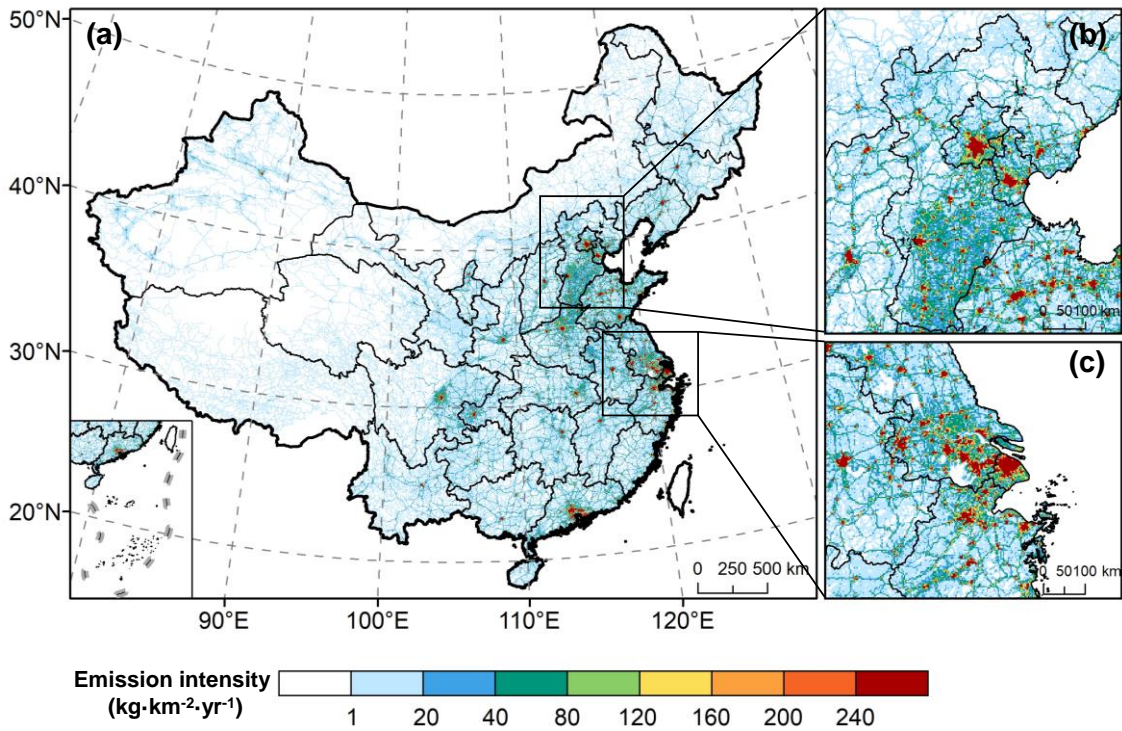
Figure 3: Spatial distribution of on-road NH₃ emission intensities in (a) mainland China, (b) the Beijing-Tianjin-Hebei (BTH) region, and (c) the Yangtze River Delta (YRD) in 2019.
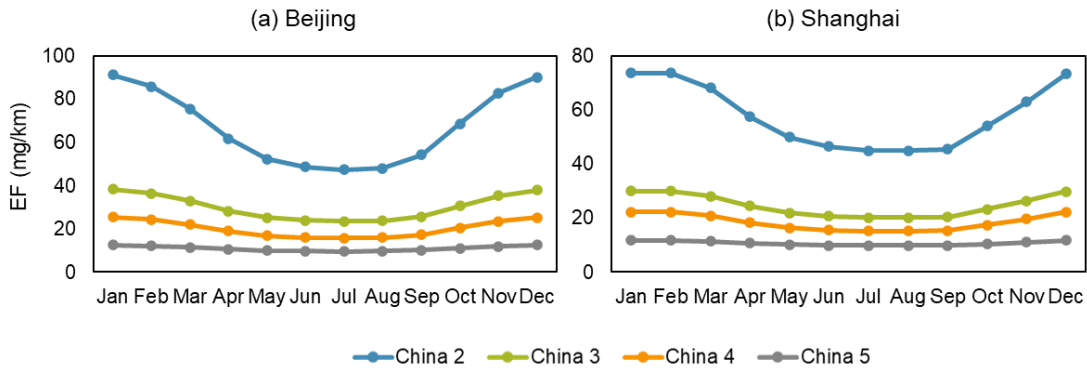
Figure 4: Monthly NH₃ EFs for LDGVs of various emission standards in (a) Beijing, and (b) Shanghai in 2019.

285
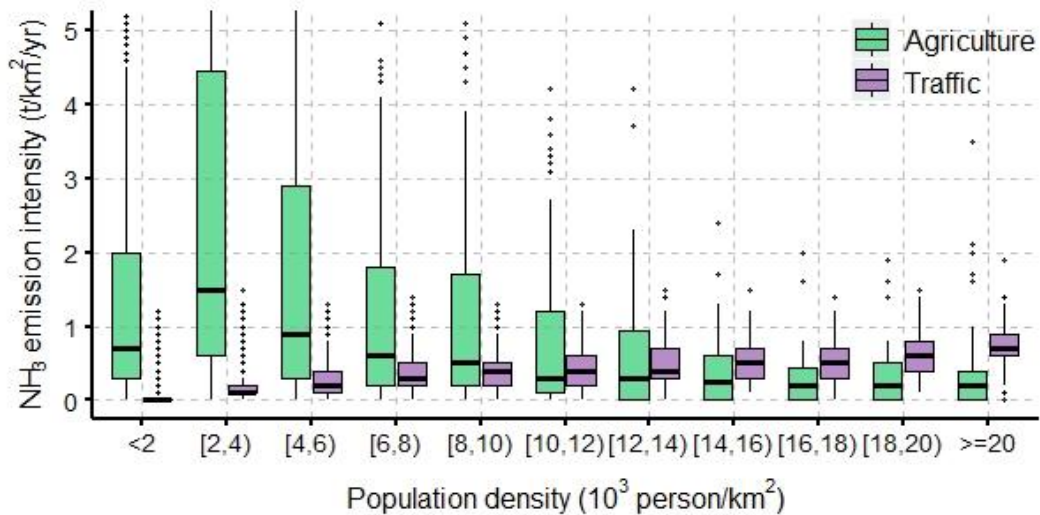
Figure 5: Distribution of agricultural and on-road NH₃ emissions among different population densities in 2019.
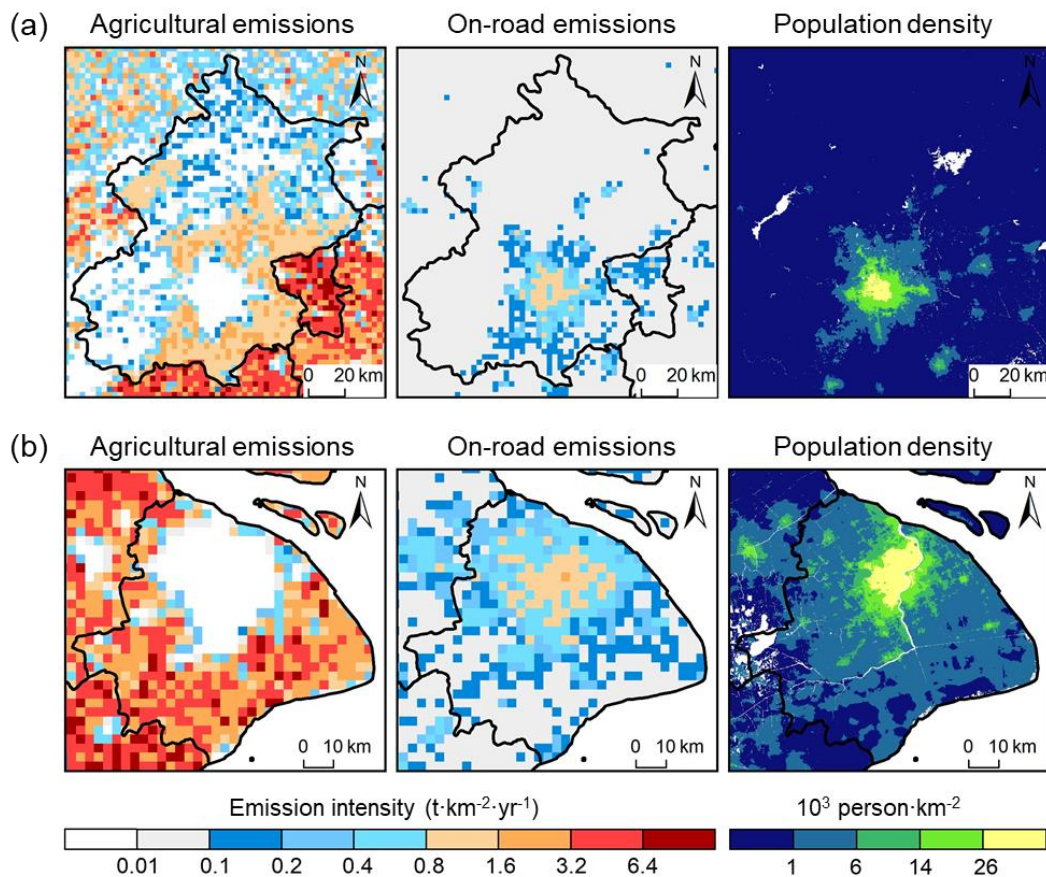
Figure 6: Spatial distributions of agricultural and on-road NH₃ emission intensities, and population density in (a) Beijing and (b) Shanghai in 2019.

Author Contributions

Yifan Wen: Data curation, Methodology, Visualization, Writing- Original draft preparation.

Shaojun Zhang: Conceptualization, Writing – review & editing, Supervision.

Ye Wu: Supervision.

Jiming Hao: Supervision.

Competing interests

The authors declare that they have no conflict of interest.

Acknowledgments

We are grateful to the National Key Research and Development Program of China (Grant No. 2022YFC3703600), the China National Postdoctoral Program for Innovative Talents (No. BX20220179) and the Shuimu Tsinghua Scholar Program (No. 2022SM011). All the authors are grateful to the Elsevier Language Editing Services for polishing the English expressions in this paper.

References

National Bureau of Statistics of China (NBSC): Annual Statistics Data of China, http://www.stats.gov.cn/enGliSH/Statisticaldata/.

An, J. Y., Huang, Y. W., Huang, C., Wang, X., Yan, R. S., Wang, Q., Wang, H. L., Jing, S. A., Zhang, Y., Liu, Y. M., Chen, Y., Xu, C., Qiao, L. P., Zhou, M., Zhu, S. H., Hu, Q. Y., Lu, J., and Chen, C. H.: Emission inventory of air pollutants and chemical speciation for specific anthropogenic sources based on local measurements in the Yangtze River Delta region, China, Atmospheric Chemistry and Physics, 21, 2003-2025, 10.5194/acp-21-2003-2021, 2021.

Bishop, G. A. and Stedman, D. H.: Reactive Nitrogen Species Emission Trends in Three Light-/Medium-Duty United States Fleets, Environ Sci Technol, 49, 11234-11240, 10.1021/acs.est.5b02392, 2015.

Bishop, G. A., Peddle, A. M., Stedman, D. H., and Zhan, T.: On-road emission measurements of reactive nitrogen compounds from three California cities, Environ Sci Technol, 44, 3616-3620, 10.1021/es903722p, 2010.

Chang, Y. H., Zou, Z., Deng, C. R., Huang, K., Collett, J. L., Lin, J., and Zhuang, G. S.: The importance of vehicle emissions as a source of atmospheric ammonia in the megacity of Shanghai, Atmospheric Chemistry and Physics, 16, 3577-3594, 10.5194/acp-16-3577-2016, 2016.

Chu, B. W., Zhang, X., Liu, Y. C., He, H., Sun, Y., Jiang, J. K., Li, J. H., and Hao, J. M.: Synergetic formation of secondary inorganic and organic aerosol: effect of SO2 and NH₃ on particle formation and growth, Atmospheric Chemistry and Physics, 16, 14219-14230, 10.5194/acp-16-14219-2016, 2016.

Davison, J., Bernard, Y., Borken-Kleefeld, J., Farren, N. J., Hausberger, S., Sjodin, A., Tate, J. E., Vaughan, A. R., and Carslaw, D. C.: Distance-based emission factors from vehicle emission remote sensing measurements, Sci Total Environ, 739, 139688, 10.1016/j.scitotenv.2020.139688, 2020.

European Commission, Directorate-General for Internal Market, I., Entrepreneurship, and SMEs: Technical studies for the development of Euro 7 : testing, pollutants and emission limits, Publications Office of the European Union, doi/10.2873/97170, 2022.

Farren, N. J., Davison, J., Rose, R. A., Wagner, R. L., and Carslaw, D. C.: Underestimated Ammonia Emissions from Road Vehicles, Environ Sci Technol, 54, 15689-15697, 10.1021/acs.est.0c05839, 2020.

325   Farren, N. J., Davison, J., Rose, R. A., Wagner, R. L., and Carslaw, D. C.: Characterisation of ammonia emissions from gasoline and gasoline hybrid passenger cars, Atmospheric Environment: X, 11, 10.1016/j.aeaoa.2021.100117, 2021.

Fenn, M. E., Bytnerowicz, A., Schilling, S. L., Vallano, D. M., Zavaleta, E. S., Weiss, S. B., Morozumi, C., Geiser, L. H., and Hanks, K.: On-road emissions of ammonia: An underappreciated source of atmospheric nitrogen deposition, Sci Total Environ, 625, 909-919, 10.1016/j.scitotenv.2017.12.313, 2018.

330   Fu, X., Wang, S., Xing, J., Zhang, X., Wang, T., and Hao, J.: Increasing Ammonia Concentrations Reduce the Effectiveness of Particle Pollution Control Achieved via SO2 and NOX Emissions Reduction in East China, Environmental Science & Technology Letters, 4, 221-227, 10.1021/acs.estlett.7b00143, 2017.

Gu, B., Zhang, L., Dingenen, R. V., Vieno, M., Grinsven, H. J. V., Zhang, X., Zhang, S., Chen, Y., Wang, S., Ren, C., Rao, S., Holland, M., Winiwarter, W., Chen, D., Xu, J., and Sutton, M. A.: Abating ammonia is more cost-effective than nitrogen oxides for mitigating PM$_{2.5}$ air
335   pollution, SCIENCE, 374, 758-762, doi:10.1126/science.abf8623, 2021.

He, L. Q., Zhang, S. J., Hu, J. N., Li, Z., Zheng, X., Cao, Y., Xu, G., Yan, M., and Wu, Y.: On-road emission measurements of reactive nitrogen compounds from heavy-duty diesel trucks in China, Environmental Pollution, 262, 114280, 10.1016/j.envpol.2020.114280, 2020.

Huang, C., Hu, Q., Lou, S., Tian, J., Wang, R., Xu, C., An, J., Ren, H., Ma, D., Quan, Y., Zhang, Y., and Li, L.: Ammonia Emission Measurements for Light-Duty Gasoline Vehicles in China and Implications for Emission Modeling, Environmental Science & Technology,
340   52, 11223-11231, 10.1021/acs.est.8b03984, 2018.

Huang, R. J., Zhang, Y. L., Bozzetti, C., Ho, K. F., Cao, J. J., Han, Y. M., Daellenbach, K. R., Slowik, J. G., Platt, S. M., Canonaco, F., Zotter, P., Wolf, R., Pieber, S. M., Bruns, E. A., Crippa, M., Ciarelli, G., Piazzalunga, A., Schwikowski, M., Abbaszade, G., Schnelle-Kreis, J., Zimmermann, R., An, Z. S., Szidat, S., Baltensperger, U., El Haddad, I., and Prevot, A. S. H.: High secondary aerosol contribution to particulate pollution during haze events in China, Nature, 514, 218-222, 10.1038/nature13774, 2014.

345   Kang, Y. N., Liu, M. X., Song, Y., Huang, X., Yao, H., Cai, X. H., Zhang, H. S., Kang, L., Liu, X. J., Yan, X. Y., He, H., Zhang, Q., Shao, M., and Zhu, T.: High-resolution ammonia emissions inventories in China from 1980 to 2012, Atmospheric Chemistry and Physics, 16, 2043-2058, 10.5194/acp-16-2043-2016, 2016.

Kong, L., Tang, X., Zhu, J., Wang, Z. F., Pan, Y. P., Wu, H. J., Wu, L., Wu, Q. Z., He, Y. X., Tian, S. L., Xie, Y. Z., Liu, Z. R., Sui, W. X., Han, L. N., and Carmichael, G.: Improved Inversion of Monthly Ammonia Emissions in China Based on the Chinese Ammonia Monitoring
350   Network and Ensemble Kalman Filter, Environmental Science & Technology, 53, 12529-12538, 2019.

Li, B. J., Chen, L., Shen, W. S., Jin, J. B., Wang, T., Wang, P. Y., Yang, Y., and Liao, H.: Improved gridded ammonia emission inventory in China, Atmospheric Chemistry and Physics, 21, 15883-15900, 10.5194/acp-21-15883-2021, 2021.

Li, Y., Schichtel, B. A., Walker, J. T., Schwede, D. B., Chen, X., Lehmann, C. M. B., Puchalski, M. A., Gay, D. A., and Collett, J. L.: Increasing importance of deposition of reduced nitrogen in the United States, Proceedings of the National Academy of Sciences of the United
355   States of America, 113, 5874-5879, 10.1073/pnas.1525736113, 2016.

Livingston, C., Rieger, P., and Winer, A.: Ammonia emissions from a representative in-use fleet of light and medium-duty vehicles in the California South Coast Air Basin, Atmospheric Environment, 43, 3326-3333, 10.1016/j.atmosenv.2009.04.009, 2009.

Lv, S., Wang, F., Wu, C., Chen, Y., Liu, S., Zhang, S., Li, D., Du, W., Zhang, F., Wang, H., Huang, C., Fu, Q., Duan, Y., and Wang, G.: Gas-to-Aerosol Phase Partitioning of Atmospheric Water-Soluble Organic Compounds at a Rural Site in China: An Enhancing Effect of
360   NH$_3$ on SOA Formation, Environ Sci Technol, 56, 3915-3924, 10.1021/acs.est.1c06855, 2022.

Mendoza-Villafuerte, P., Suarez-Bertoa, R., Giechaskiel, B., Riccobono, F., Bulgheroni, C., Astorga, C., and Perujo, A.: NOx, NH$_3$, N$_2$O and PN real driving emissions from a Euro VI heavy-duty vehicle. Impact of regulatory on-road test conditions on emissions, Sci Total Environ, 609, 546-555, 10.1016/j.scitotenv.2017.07.168, 2017.

Meng, W., Zhong, Q., Yun, X., Zhu, X., Huang, T., Shen, H., Chen, Y., Chen, H., Zhou, F., Liu, J., Wang, X., Zeng, E. Y., and Tao, S.:
365   Improvement of a Global High-Resolution Ammonia Emission Inventory for Combustion and Industrial Sources with New Data from the Residential and Transportation Sectors, Environ Sci Technol, 51, 2821-2829, 10.1021/acs.est.6b03694, 2017.

OpenStreetMap: OpenStreetMap data for China, 2022.

Pan, Y., Tian, S., Liu, D., Fang, Y., Zhu, X., Zhang, Q., Zheng, B., Michalski, G., and Wang, Y.: Fossil Fuel Combustion-Related Emissions Dominate Atmospheric Ammonia Sources during Severe Haze Episodes: Evidence from (15)N-Stable Isotope in Size-Resolved Aerosol
370   Ammonium, Environ Sci Technol, 50, 8049-8056, 10.1021/acs.est.6b00634, 2016.

Pandolfi, M., Amato, F., Reche, C., Alastuey, A., Otjes, R. P., Blom, M. J., and Querol, X.: Summer ammonia measurements in a densely populated Mediterranean city, Atmos. Chem. Phys., 12, 7557-7575, 10.5194/acp-12-7557-2012, 2012.

Paulot, F., Jacob, D. J., Pinder, R. W., Bash, J. O., Travis, K., and Henze, D. K.: Ammonia emissions in the United States, European Union, and China derived by high-resolution inversion of ammonium wet deposition data: Interpretation with a new agricultural emissions inventory
375   (MASAGE_NH$_3$), J Geophys Res-Atmos, 119, 4343-4364, 2014.

Plautz, J.: Piercing the haze, 361, 1060-1063, doi:10.1126/science.361.6407.1060, 2018.

Ru-Jin, H., Yanlin, Z., Carlo, B., Kin-Fai, H., Jun-Ji, C., Yongming, H., Daellenbach, K. R., Slowik, J. G., Platt, S. M., and Francesco, C.: High secondary aerosol contribution to particulate pollution during haze events in China, Nature, 514, 218-222, 2014.

Selleri, T., Melas, A., Bonnel, P., and Suarez-Bertoa, R.: NH$_3$ and CO Emissions from Fifteen Euro 6d and Euro 6d-TEMP Gasoline-Fuelled
380   Vehicles, Catalysts, 12, 245, 2022.

Sha, Z. P., Liu, H. J., Wang, J. X., Ma, X., Liu, X. J., and Misselbrook, T.: Improved soil-crop system management aids in NH$_3$ emission mitigation in China, Environmental Pollution, 289, ARTN 117844 10.1016/j.envpol.2021.117844, 2021.

Streets, D., Bond, T., Carmichael, G., Fernandes, S., Fu, Q., He, D., Klimont, Z., Nelson, S., Tsai, N. Y., Wang, M., Woo, J., and Yarber, K.: An inventory of gaseous and primary aerosol emissions in Asia in the year 2000, J Geophys Res-Atmos, 108, 10.1029/2002jd003093, 2003.

Stevens, C. J., Dise, N. B., Mountford, J. O., and Gowing, D. J.: Impact of nitrogen deposition on the species richness of grasslands, Science, 303, 1876-1879, DOI 10.1126/science.1094678, 2004.

Suarez-Bertoa, R., Mendoza-Villafuerte, P., Riccobono, F., Vojtisek, M., Pechout, M., Perujo, A., and Astorga, C.: On-road measurement of NH$_3$ emissions from gasoline and diesel passenger cars during real world driving conditions, Atmospheric Environment, 166, 488-497, 10.1016/j.atmosenv.2017.07.056, 2017.

Sun, K., Tao, L., Miller, D. J., Pan, D., Golston, L. M., Zondlo, M. A., Griffin, R. J., Wallace, H. W., Leong, Y. J., Yang, M. M., Zhang, Y., Mauzerall, D. L., and Zhu, T.: Vehicle Emissions as an Important Urban Ammonia Source in the United States and China, Environmental Science & Technology, 51, 2472-2481, 10.1021/acs.est.6b02805, 2017a.

Sun, K., Tao, L., Miller, D. J., Pan, D., Golston, L. M., Zondlo, M. A., Griffin, R. J., Wallace, H. W., Leong, Y. J., Yang, M. M., Zhang, Y., Mauzerall, D. L., and Zhu, T.: Vehicle Emissions as an Important Urban Ammonia Source in the United States and China, Environ Sci Technol, 51, 2472-2481, 10.1021/acs.est.6b02805, 2017b.

Tatem, A. J.: WorldPop, open data for spatial demography, Sci Data, 4, 170004, 10.1038/sdata.2017.4, 2017.

Torp, T. K., Hansen, B. B., Vennestrøm, P. N. R., Janssens, T. V. W., and Jensen, A. D.: Modeling and Optimization of Multi-functional Ammonia Slip Catalysts for Diesel Exhaust Aftertreatment, Emission Control Science and Technology, 7, 7-25, 10.1007/s40825-020-00183-x, 2021.

Wang, S., Nan, J., Shi, C., Fu, Q., Gao, S., Wang, D., Cui, H., Saiz-Lopez, A., and Zhou, B.: Atmospheric ammonia and its impacts on regional air quality over the megacity of Shanghai, China, Scientific Reports, 5, 15842, 10.1038/srep15842, 2015.

Wang, Y., Wen, Y., Zhang, S., Zheng, G., Zheng, H., Chang, X., Huang, C., Wang, S., Wu, Y., and Hao, J.: Vehicular Ammonia Emissions Significantly Contribute to Urban PM2.5 Pollution in Two Chinese Megacities, Environmental Science & Technology, 57, 2698-2705, 10.1021/acs.est.2c06198, 2023.

Wen, Y., Zhang, S., He, L., Yang, S., Wu, X., and Wu, Y.: Characterizing start emissions of gasoline vehicles and the seasonal, diurnal and spatial variabilities in China, Atmospheric Environment, 245, 118040, https://doi.org/10.1016/j.atmosenv.2020.118040, 2021.

Wen, Y., Wu, R., Zhou, Z., Zhang, S., Yang, S., Wallington, T. J., Shen, W., Tan, Q., Deng, Y., and Wu, Y.: A data-driven method of traffic emissions mapping with land use random forest models, Applied Energy, 305, 10.1016/j.apenergy.2021.117916, 2022a.

Wen, Y. F., Zhang, S. J., Zhang, J. R., Bao, S. H., Wu, X. M., Yang, D. Y., and Wu, Y.: Mapping dynamic road emissions for a megacity by using open-access traffic congestion index data, Applied Energy, 260, 114357, ARTN 114357 10.1016/j.apenergy.2019.114357, 2020.

Wen, Y. F., Wu, R. X., Zhou, Z. H., Zhang, S. J., Yang, S. G., Wallington, T. J., Shen, W., Tan, Q. W., Deng, Y., and Wu, Y.: A data-driven method of traffic emissions mapping with land use random forest models, Applied Energy, 305, 117916, 2022b.

World Development Indicators: http://wdi.worldbank.org/table/3.12, last access: 2022-03-20.

Wu, X., Wu, Y., Zhang, S., Liu, H., Fu, L., and Hao, J.: Assessment of vehicle emission programs in China during 1998-2013: Achievement, challenges and implications, Environ Pollut, 214, 556-567, 10.1016/j.envpol.2016.04.042, 2016.

Wu, Y., Zhang, S., Hao, J., Liu, H., Wu, X., Hu, J., Walsh, M. P., Wallington, T. J., Zhang, K. M., and Stevanovic, S.: On-road vehicle emissions and their control in China: A review and outlook, Sci Total Environ, 574, 332-349, 10.1016/j.scitotenv.2016.09.040, 2017a.

Wu, Y., Zhang, S., Hao, J., Liu, H., Wu, X., Hu, J., Walsh, M. P., Wallington, T. J., Zhang, K. M., and Stevanovic, S.: On-road vehicle emissions and their control in China: A review and outlook, Science of the Total Environment, 574, 332-349, 2017b.

Xing, J., Pleim, J., Mathur, R., Pouliot, G., Hogrefe, C., Gan, C. M., and Wei, C.: Historical gaseous and primary aerosol emissions in the United States from 1990 to 2010, Atmospheric Chemistry and Physics, 13, 7531-7549, 10.5194/acp-13-7531-2013, 2013.

Xu, X., Liu, J., Zhang, S., Li, R., Yan, C., Wu, S. J. R., and Environment Data Cloud Platform: Beijing, C.: China's multi-period land use land cover remote sensing monitoring data set (CNLUCC), 10.12078/2018070201, 2018.

Yang, D. Y., Zhang, S. J., Niu, T. L., Wang, Y. J., Xu, H. L., Zhang, K. M., and Wu, Y.: High-resolution mapping of vehicle emissions of atmospheric pollutants based on large-scale, real-world traffic datasets, Atmospheric Chemistry and Physics, 19, 8831-8843, 10.5194/acp-19-8831-2019, 2019.

Zhang, L., Chen, Y. F., Zhao, Y. H., Henze, D. K., Zhu, L. Y., Song, Y., Paulot, F., Liu, X. J., Pan, Y. P., Lin, Y., and Huang, B. X.: Agricultural ammonia emissions in China: reconciling bottom-up and top-down estimates, Atmospheric Chemistry and Physics, 18, 339-355, 10.5194/acp-18-339-2018, 2018.

Zhang, S., Wu, Y., Wu, X., Li, M., Ge, Y., Liang, B., Xu, Y., Zhou, Y., Liu, H., Fu, L., and Hao, J.: Historic and future trends of vehicle emissions in Beijing, 1998–2020: A policy assessment for the most stringent vehicle emission control program in China, Atmospheric Environment, 89, 216-229, 10.1016/j.atmosenv.2013.12.002, 2014.

Zhao, B., Wang, P., Ma, J. Z., Zhu, S., Pozzer, A., and Li, W.: A high-resolution emission inventory of primary pollutants for the Huabei region, China, Atmospheric Chemistry and Physics, 12, 481-501, 10.5194/acp-12-481-2012, 2012.

Zheng, H., Zhao, B., Wang, S., Wang, T., Ding, D., Chang, X., Liu, K., Xing, J., Dong, Z., Aunan, K., Liu, T., Wu, X., Zhang, S., and Wu, Y.: Transition in source contributions of PM2.5 exposure and associated premature mortality in China during 2005–2015, Environment International, 132, 105111, https://doi.org/10.1016/j.envint.2019.105111, 2019.

Zheng, J. Y., Yin, S. S., Kang, D. W., Che, W. W., and Zhong, L. J.: Development and uncertainty analysis of a high-resolution NH_3 emissions inventory and its implications with precipitation over the Pearl River Delta region, China, Atmospheric Chemistry and Physics, 12, 7041-7058, 10.5194/acp-12-7041-2012, 2012.

440